Forest Ecology and Management 259 (2010) 2342–2354

Contents lists available at ScienceDirect

Forest Ecology and Management

journal homepage: www.elsevier.com/locate/foreco

Pre-impact forest composition and ongoing tree mortality associated with sudden oak death in the Big Sur region; California

Frank W. Davis[a,*], Mark Borchert[b], Ross K. Meentemeyer[c], Alan Flint[d], David M. Rizzo[e]

[a] Bren School of Environmental Science and Management, University of California, Santa Barbara, CA 93106-5131, USA
[b] San Bernardino National Forest, San Bernardino, CA 92408, USA
[c] Department of Geography and Earth Science, University of North Carolina, Charlotte, NC 28223, USA
[d] U.S. Geological Survey, California Water Sciences Center, Sacramento, CA 95819, USA
[e] Department of Plant Pathology, University of California, Davis, CA 95616, USA

ARTICLE INFO

Article history:
Received 24 November 2009
Received in revised form 10 March 2010
Accepted 12 March 2010

Keywords:
Species distribution models
Landscape disease pattern
Community ordination
Spatial autocorrelation
Chaparral

ABSTRACT

Mixed-evergreen forests of central coastal California are being severely impacted by the recently introduced plant pathogen, *Phytophthora ramorum*. We collected forest plot data using a multi-scale sampling design to characterize pre-infestation forest composition and ongoing tree mortality along environmental and time-since-fire gradients. Vegetation pattern was described using trend surface analysis, spatial autocorrelation analysis and redundancy analysis. Species-environment associations were modeled using non-parametric multiplicative regression (NPMR). Tanoak (*Lithocarpus densiflorus*) mortality was analyzed with respect to environmental and biotic factors using trend surface analysis and multivariate regression. Mixed-evergreen forest occurs throughout the Big Sur region but is most widespread in the north, on north facing slopes, at mid-elevations near the coast. Relative basal area of the dominant tree species changes fairly predictably from north to south and from coast to interior in relation to mapped patterns of precipitation, temperature factors and soil characteristics. Most dominant tree species sprout vigorously after fire. The forests experience a mixed-fire regime in this region ranging from low severity understory burns to high severity crown fires, with the latter increasing above the marine inversion layer and at more interior locations. *Ceanothus* spp. can dominate mixed-evergreen sites for several decades after severe fires. All of the dominant broadleaf evergreen tree species are hosts of *P. ramorum*, although not all will die from infection. Tanoak mortality decreases from northwest to southeast and is significantly correlated with climate, especially growing degree days and mean annual precipitation, and with basal area of the foliar host bay laurel (*Umbellularia californica*) in a 0.5–1 ha neighborhood. Adaptive management of mixed-evergreen forest to mitigate *P. ramorum* impacts in the region will need to consider large local and regional variation in forest composition and the potentially strong interactions between climate, fire, forest composition and disease severity.

1. Introduction

Exotic plant pathogens are important agents of forest change in many regions around the globe (Castello et al., 1995; Hall et al., 2002; Loo, 2009). The spread and consequences of these pathogens regulate and are regulated by landscape patterns in biophysical environments (White et al., 2002), forest structure and composition (Perkins and Matlack, 2002; Condeso and Meentemeyer, 2007), and disturbance processes such as fire (Holzmueller et al., 2008) and landslides (Johnson and Wilcock, 2002). For example, Perkins and Matlack (2002) demonstrated that spread of fusiform rust (causal agent *Cronartium quercuum*) is promoted by the high level of connectivity of pine plantations in the southeastern United States. Condeso and Meentemeyer (2007) found that the severity of sudden oak death (causal agent *Phytopthora ramorum*) in mixed-evergreen forests of northern California was greater in plots surrounded by a high proportion of contiguous forest. Understanding landscape patterns and controls on forest composition in relation to disease dynamics is an important component of developing management strategies to cope with forest disease outbreaks (Holdenrieder et al., 2004; Chornesky et al., 2005).

Since its discovery in the San Francisco Bay area of California in the mid-1990s, *P. ramorum*, the causal agent of the forest disease known as "Sudden Oak Death" (SOD), has killed millions of tanoaks (*Lithocarpus densiflorus*, recently attributed to a new genus *Notholithocarpus densiflorus*) and oaks (*Quercus* spp.) in the mixed broadleaf evergreen forests ("mixed-evergreen forests") and redwood forests of coastal California (Meentemeyer et al., 2008c). *P.*

* Corresponding author. Tel.: +1 805 893 3438; fax: +1 805 893 7612.
E-mail address: fwd@icess.ic.ucsb.edu (F.W. Davis).

0378-1127/$ – see front matter © 2010 Elsevier B.V. All rights reserved.
doi:10.1016/j.foreco.2010.03.007

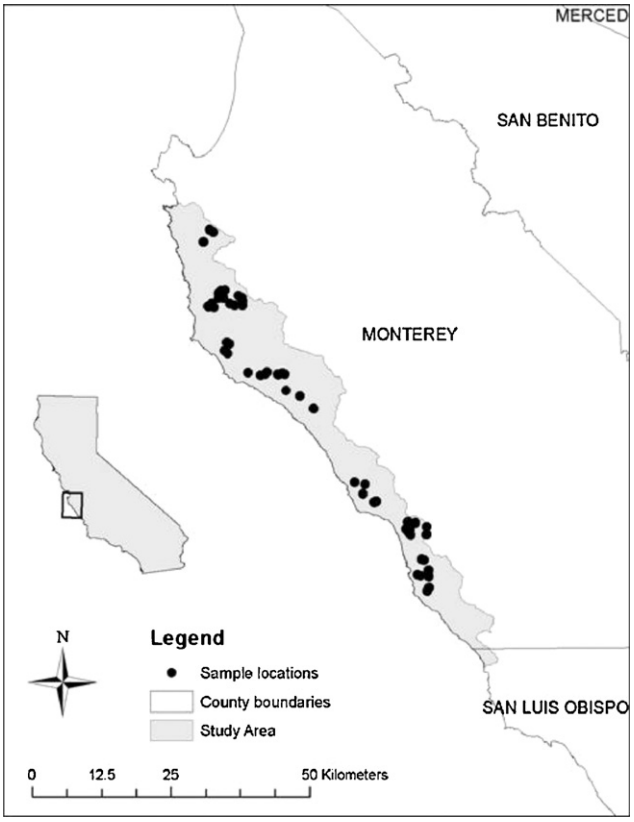

Fig. 1. Map of the study area (shaded) with inset showing the areas's location in California. Dots indicate sites for clustered sampling of forest structure and composition.

ramorum is now established in coastal forests from the Big Sur coast northward to southern Mendocino County; disjunct introductions have also been detected in southern Humboldt County and Curry County, Oregon.

P. ramorum infects at least 30 native California woody and herbaceous host species, causing non-lethal foliar and twig damage in some species (e.g., California bay laurel, *Umbellularia californica*) and lethal twig and stem cankers in others (notably some Fagaceae) (Rizzo and Garbelotto, 2003). Among canker-forming hosts, tanoak is especially susceptible to infection and subsequent mortality; basal area and tree density reductions of over 50% have been observed in monitored tanoak stands within 8 years of initial infestation (Waring and O'Hara, 2008). Annual mortality rates of 4.5–5.5% (an order of magnitude higher than background rates) have also occurred in coast live oak (*Quercus agrifolia*) populations in infested areas (Brown and Allen-Diaz, 2009). Other tree species that may be killed by *P. ramorum* in California include Shreve oak (*Q. parvula var. shrevei*), black oak (*Q. kelloggii*), canyon live oak (*Q. chrysolepis*) and madrone (*Arbutus menziesii*), all of which are important members of mixed-evergreen forest communities (Rizzo and Garbelotto, 2003). The immediate and long term impacts of *P. ramorum*-associated mortality on California mixed-evergreen forests are not well understood, in part because of the relatively short time since the pathogen was introduced, but also because of the limited ecological research on mixed-evergreen forest composition and dynamics (Rizzo and Garbelotto, 2003).

Forests in the Big Sur region (Fig. 1) are among the most impacted by *P. ramorum* (Meentemeyer et al., 2008b). Due to disease-associated tree mortality, mixed-evergreen forests here are undergoing rapid, large scale changes in overstory composition and structure that could have cascading effects on multi-scale vegetation pattern and composition, and associated ecosystem and

Fig. 2. Example of fine-grained vegetation on the Big Sur Coast. Mixed-evergreen forest (rough-textured patches) occurs in a patchwork with coast redwood forests, grassland, coastal scrub and chaparral. Image is oriented north-south and 5 km across.

disturbance processes. However, the ecology of coastal mixed-evergreen forests has not been well characterized (Davis and Borchert, 2006).

Mixed-evergreen forest in Big Sur is patchily distributed in complex, fine-grained vegetation mosaics of coast redwood (*Sequoia sempervirens*) forest, coastal sage scrub, annual grassland and chaparral (Fig. 2). Forest composition turns over rapidly as one moves upslope and away from the coast along steep gradients in maritime influence and orographic precipitation that interact with soil topomosaics and fire history (Cooper, 1922; Wells, 1962; Sawyer et al., 1977; Davis and Borchert, 2006). As a result of *P. ramorum*'s rapid spread and establishment, we are currently in a narrow window of time where it is still possible to characterize pre-infestation forest composition and dynamics in relation to the spread and impacts of the disease. This information will be critical in setting priorities and goals leading to potential disease management decisions. In particular, we lack quantitative information on how host tree species' distributions vary across local-to-regional scales, the association of host species distributions with site factors and fire history, and the current scale-dependent pattern of tree mortality in relationship to forest composition and environmental factors.

We sampled mixed-evergreen forests of the Big Sur Coast, focusing on stands co-dominated by tanoak, to answer the following questions:

- How does forest composition vary across the Big Sur region in relation to location, environmental gradients and fire history?
- How does basal area of dominant tree species vary as a function of spatial scale, environmental factors and fire history?

Although our research focused on characterizing pre-infestation forest composition and dynamics, because we measured both dead and live basal area we also considered two additional questions.

- How has recent SOD-associated tree mortality affected spatial pattern and composition of mixed-evergreen forest?
- How does the current level of forest dieback – in particular the dieback of tanoak – vary as a function of relative abundance of other host tree species, climate, topography, soils and fire history?

Based on previous research, our study design and statistical analyses were guided by the following premises:

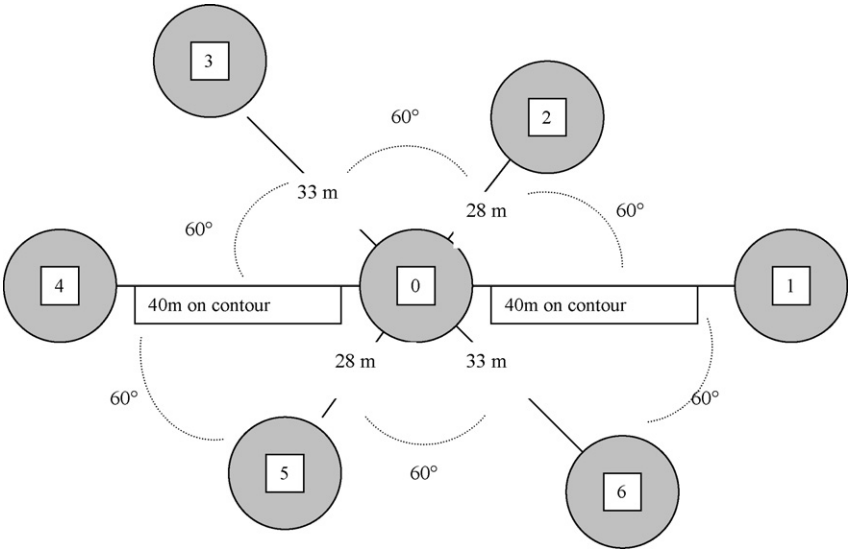

Fig. 3. Layout of variable radius basal area plots at a stratified random sample of sites across the study region. The layout was designed to provide a large number of short and intermediate inter-plot distances along and across local hillslope gradients for spatial autocorrelation analysis.

- Relative abundance of dominant tree species in coastal California is principally controlled by local gradients in soil moisture (Cooper, 1922; Waring and Major, 1964). These gradients in turn are controlled by factors operating at multiple scales ranging from local climate to local and microscale variation in soil properties, hillslope hydrology and surface energy balance.
- Forest structure and composition vary over short distances in relation to local topography and drainage and as a result of fine-scale disturbance processes such as soil slumping and tree throw (Cooper, 1922; Hunter and Parker, 1993; Condeso and Meentemeyer, 2007).
- *P. ramorum* infection levels increase locally with increasing relative abundance of host trees, especially bay laurel (*U. californica*), and cooler understory temperatures (Davidson et al., 2008; Meentemeyer et al., 2008b; Cobb et al., 2010). Disease incidence increases regionally in wetter and more coastal settings (Meentemeyer et al., 2004, 2008a).

Published research and ongoing studies provide ample evidence associating *P. ramorum* with forest dieback in the Big Sur region. Our objective is to improve understanding of the host community and the interplay of variation in host tree abundance and environmental gradients with forest dieback during this relatively early stage of progression of the pathogen across the region.

2. Study area and methods

2.1. Data collection

We sampled mixed-evergreen forest in the northern Santa Lucia Mountains from Carmel Bay south to the Willow Creek drainage in the Big Sur region of Monterey County, CA (W 121°56′, N 36°31′ to W 121°18′, N 35°46′, Fig. 1). The region is mainly underlain by Mesozoic granitic and Pre-Cretaceous metamorphic rock, but also contains areas of Miocene marine sedimentary sandstones and shales (Miles and Goudey, 1997). Mean annual precipitation declines gradually from north to south and ranges from 65 cm near the coast to >130 cm at elevations above 1450 m a few km inland (Davis and Borchert, 2006). At coastal stations, mean monthly temperatures at sea level range from 10–13 °C in the winter months to 16–18 °C in the summer. The cool ocean surface creates a steep summer marine inversion associated with coastal fog and rapid temperature increases with elevation to the top of the inversion layer at around 300–500 m during summer months. Coastal mountains prevent the marine influence from reaching more than a few kilometers inland from the coast except via large river valleys; inland temperature regimes are considerably more continental. Soils are mostly shallow orthisols and xerisols (Miles and Goudey, 1997). Vegetation is a complex mosaic of grasslands, shrublands and forests (Fig. 2). Coastal plain and foothills generally support coastal prairie, annual grassland, coastal sage scrub, maritime chaparral, closed cone pine forests, and coast redwood forest in ravines and river valleys. The lower montane zone supports topo-mosaics of chaparral, coastal sage scrub, and mixed-evergreen forest. Higher elevations support mixed-evergreen forest, pine woodlands and mixed-conifer forests.

Between March and June 2006 we established 58 sampling sites ("sites") centered on a subset of 280 permanent plots established by the Big Sur Ecoregion Sudden Oak Death Adaptive Management Project (SOD-AMP) (Wickland et al., 2008) (Fig. 1). The 280 SOD-AMP permanent plots were located using a stratified random design based on seven watersheds, forest type (redwood forest vs. mixed-evergreen forest), three levels of tree mortality, and public vs. private land ownership. *P. ramorum* was confirmed via culturing on 153 of the 280 plots. We sampled a subset of SOD-AMP plots within the mixed-evergreen forest stratum across all watersheds, selecting plots to span a coast-to-interior gradient having a wide range of fire histories from recently burned to long unburned plots. We did not apply any pre-existing system of community associations or forest types, but because of our interest in tanoak mortality we sampled a disproportionate number of SOD-AMP plots with tanoak present. Plots were located using waypoints in a handheld GPS. In a few cases we randomly re-located plots in the same neighborhood when computer-generated locations were inaccessible or fell in vegetation types other than mixed-evergreen forest.

We clustered sample plots at each site using an array of 7 variable radius basal area plots centered on the SOD-AMP plot (Fig. 3). The array was designed to sample local variation in forest structure and composition, with three plots oriented along the elevation contour, two upslope plots and two downslope plots at 28–40 m from the central point. Twelve plots were removed because they landed in inaccessible or road-affected areas, and at two locations we added two additional plots, resulting in a total of 399 plots. One

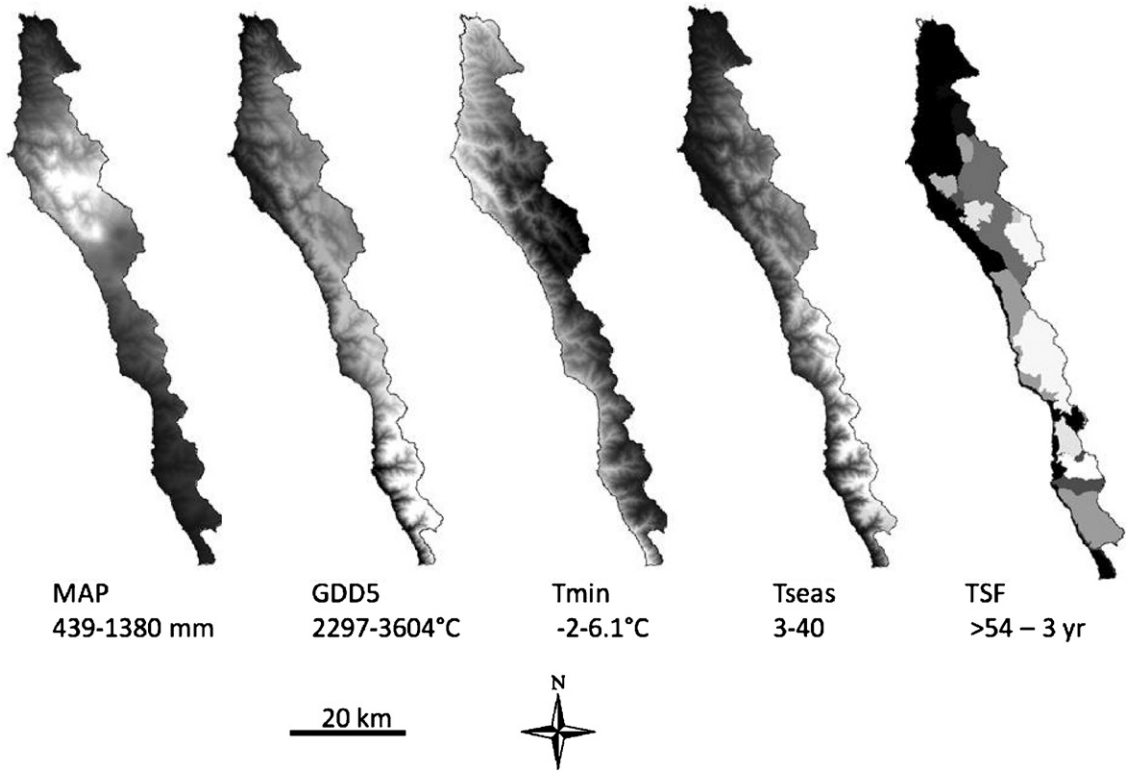

Fig. 4. Maps of 90 m grids of environmental variables used to predict mixed-evergreen forest composition including mean annual precipitation (MAP), growing degree days above 5 °C (GDD5), average minimum daily temperature of the coldest month (T_{min}), temperature seasonality (T_{seas}) and time since fire (TSF). The ranges of values indicate the scaling from low (black) to high (white) in the grayscale maps.

outlier plot of pure Coulter pine (*Pinus coulteri*) was also removed from further analysis for a final data set of 398 plots.

At each of the 398 plots we measured basal area for each tree species using a Spiegel Relaskop (Finch, 1957). A basal area factor of 20 ensured that all but the largest redwoods were not counted in more than one plot. Many plots included recently killed standing and downed trees that were readily identifiable to species. We tallied all trees and coded each stem as live, standing dead, or downed and dead. We also recorded the diameter at breast height (dbh) of each tallied stem in 5 cm classes. At the center plot we used a handheld GPS to record geographic location and elevation (5–10 m accuracy). Geographic coordinates of the other plots in the array were calculated based on distance, direction and vertical angle from the center plot. At every plot we recorded local slope angle and aspect. Plot-level basal area data were averaged to obtain site-level data.

We examined vegetation–climate associations using 90 m resolution grids of recent historical climate variables. Grids of historical climate at a monthly time step were produced by downscaling monthly 4 km PRISM climate data (Daly et al., 2008) for the period 1971–2000. Downscaling was accomplished with 90 m digital elevation grids using a modified gradient-inverse-distance square interpolation method (Flint and Flint, 2007). The method preserves the structure of the coarser PRISM grids and uses 90 m digital

Table 1
Correlation matrix for environmental variables at plot scale ($n = 398$) and site-scale ($n = 58$). Site-scale correlations are in parentheses.

Variable	Variable name	Flow	AWC	TSF	MAP	MinT	GDD5	T_{seas}	Heat
Soil available water holding capacity, 0–100 cm	AWC	0.09 (0.03)							
Time since fire (yrs)	TSF	−0.12 (−0.19)	−0.07 (−0.01)						
Mean annual precipitation (mm)	MAP	−0.09 (−0.14)	−0.41 (−0.40)	−0.06 (−0.06)					
Minimum temperature (0.1 °C)	MinT	0.05 (0.07)	0.06 (−0.11)	−0.27 (−0.27)	−0.14 (−0.16)				
Growing degree days above 5 °C	GDD5	0.21 (0.27)	0.29 (0.29)	−0.08 (−0.07)	−0.68 (−0.68)	0.21 (0.23)			
Temperature seasonality (0–100)	T_{seas}	0.05 (0.08)	0.12 (0.28)	−0.29 (−0.28)	−0.24 (−0.23)	−0.84 (−0.84)	0.29 (0.29)		
Annual heat load (unitless)	Heat	0.02 (0.20)	0.00 (0.05)	0.01 (−0.03)	0.05 (−0.10)	−0.09 (−0.10)	−0.14 (0.06)	0.10 (0.19)	
Annual direct solar radiation ln(MJ cm^{-2} yr^{-1})	Solar	−0.02 (0.09)	0.09 (0.17)	0.02 (0.02)	−0.11 (−0.10)	−0.28 (−0.31)	−0.11 (−0.14)	0.32 (0.34)	0.51 (0.55)

elevation data for additional topographic downscaling. We tested climate variables known to be important factors affecting phenology and growth of western trees species (Rehfeldt et al., 2006). This included mean annual precipitation (mm) and three temperature related variables: growing degree days above 5 °C (Rehfeldt et al., 2006), average minimum daily temperature of the coldest month (0.1 °C) and temperature seasonality (Fig. 4). Annual growing degree days above 5 °C is estimated as

$$GDD5 = \sum_{i=1}^{12} \left[\left(\frac{T_{\min_i} + T_{\max_i}}{2} - 5 \right) D_i \right] \quad (1)$$

where $T_{\min}$ and $T_{\max}$ are average daily minimum and maximum temperatures for month i and D is the number of days in month i. When $T_{\min_i} < 5\,^{\circ}\mathrm{C} < T_{\max_i}$, we adjust the number of days using $D_i^* = D_i(T_{\max} - 5)/(T_{\max} - T_{\min})$.

Temperature seasonality was calculated as the standard deviation of monthly mean temperatures rescaled from 0 to 100 for the range of values observed in California.

We also analyzed local topographic factors known to be associated with species distributions including solar radiation, annual heat load, and a topographic moisture index. Potential annual direct incident solar radiation and annual heat load were calculated from field-measured slope and aspect using equations provided by McCune (2007). A topographic moisture index (Moore et al., 1991) was calculated as ln(flow.accum/tan β), where β is the local slope angle and flow.accum is watershed area draining through the site as calculated using the flow accumulation tool in ArcGIS and 28 m shuttle radar digital elevation data (Farr et al., 2007). Plot data were averaged to obtain site-level estimates of topographic variables.

Time-since-burning was estimated for each plot based on fire history maps maintained by the California Department of Forestry and Fire Protection (Cal Fire, 2006; Fig. 4). Soil type (Series and Phase) and associated physical properties such as available water holding capacity of the upper 50 cm were assigned to plots by GIS overlay of plot locations on SSURGO soil maps that have a minimum mapping unit scale of 2–12 ha (USDA-NRCS, 2004).

Most environmental factors were only moderately correlated at plot and site-scales ($r < 0.30$, Table 1). Exceptions included high correlations between mean annual precipitation and growing degree days ($r = -0.68$), minimum temperature and temperature seasonality ($r = -0.84$), and annual solar radiation and annual heat load ($r = 0.55$). Deeper soils with high available water holding capacity occur at lower elevations closer to the coast and are thus negatively correlated with precipitation ($r = -0.41$). Time since fire generally decreases further from the coast with more continental climate and is negatively correlated with minimum temperature and temperature seasonality.

2.2. Data analysis

2.2.1. Host species' distributions and environmental associations

We compared the distributions of environmental factors in central plots at the 58 sites to the distributions from the larger set of 280 SOD-AMP mixed-evergreen forest sites using two-sample t-tests to test for sampling bias in our site locations relative to average conditions for mixed-evergreen forests in the region, We compared the fire history of our 398 sample plots to the fire history for the region as a whole.

Spatial scale-dependence of vegetation pattern was described with Mantel correlograms showing the correlation of plot compositional dissimilarity as a function of separation distance. Species data were first de-trended using redundancy analysis with geographic northing and easting as explanatory variables to remove a modest northwest-southeast trend in vegetation composition (Borcard et al., 2004). Compositional dissimilarity was measured with the Hellinger distance metric, which measures the Euclidean distance between plots after a square root transform of species relative abundances in the plot (Legendre and Gallagher, 2001). The Hellinger distance downweights rare species and performs well over long compositional gradients with associated sparse data matrices (Legendre and Gallagher, 2001). Separate multivariate spatial correlograms based on total tree basal area and live tree basal area were produced using the *ecodist* package in *R* (Goslee and Urban, 2007). Significance testing was based on 1000 permutations of one of the distance matrices.

Vegetation–environment relationships were investigated at the plot ($n = 398$) scale, which was finer than the scale of climate data and at the scale of topographic variables. Unless otherwise noted, we analyzed total live plus recently dead basal area for all species. Redundancy analysis (RDA) of the Hellinger-transformed plot-by-species matrix (Legendre and Gallagher, 2001) was performed using the program *rda* in the *vegan* package in *R*. RDA is a constrained ordination method in which species data are regressed against environmental factors and the regression predictions are subjected to principal components analysis. Environmental factors for RDA analysis were selected based on forward and backward selection of a multivariate dependent variable based on p-values from 1000 permutations. The procedure was implemented using the *ordistep* function in the *vegan* package in *R* (Blanchet et al., 2008).

2.2.2. Species–environment associations and species distribution models

Site-level species–soil associations were tested using simple chi-square analysis of species presence–absence data. We recognize the potential circularity in associating vegetation type with mapped soil type and associated variables such as soil depth and available water holding capacity, given that vegetation pattern may have guided soil mapping. We assume this circularity is of less concern in analyzing the distributions of individual tree species within the mixed-evergreen forest type, but have avoided the issue in multivariate models described below by excluding mapped soil factors.

We modeled species' associations with climatic and topographic factors at the site-scale using non-parametric multiplicative regression (NPMR) (McCune, 2006). Like generalized additive models (Hastie and Tibshirani, 1986), NPMR applies a kernel smoothing function to predictor data, but variable weights are multiplied rather than added to allow for strong interactions among predictor variables in relation to species responses. Model selection is based on minimizing residual sum of squares; leave-one-out cross-validation is applied to reduce the risk of over-fitting the data. The mean residual sum of squares or "pseudo-R^2" is used to evaluate model goodness-of-fit.

We fitted separate NPMR models for each species using Gaussian (local mean) kernels, and iterative model building with a forward stepwise selection procedure based on pseudo-R^2. Best 1-, 2- and 3-factor non-parametric multiplicative regression models were tabulated and visually compared using the program *Hyperniche* (McCune and Mefford, 2004).

To help interpet the NPMR models, 90 m raster maps of predicted relative basal area were produced for each species using *Hyperniche* and 90 m grids of climate variables. Topographic factors such as solar radiation and annual heatload were calculated using 28 m elevation grids and then re-scaled to 90 m using bi-linear interpolation.

2.2.3. Disease impacts: regional patterns of tanoak mortality

We assume but did not confirm through lab cultures that *P. ramorum* was responsible for all recent tree mortality in our sample plots; however a subset of trees in and around the plots were

Table 2
Frequency, mean basal area, and dead basal area as a proportion of total basal areas, for all woody species tallied in 398 plots. Species are sorted from highest to lowest frequency in 398 plots.

Common name (Abbreviation)	Species	Frequency (n = 398)	Mean basal area (m^2/ha)	Proportion dead basal area
Tanoak (LIDE)	*Lithocarpus densiflorus*	0.590	13.84	0.263
Redwood (SESE)	*Sequoia sempervirens*	0.458	12.72	0.011
California bay (UMCA)	*Umbellularia californica*	0.427	7.79	0.068
Madrone (ARME)	*Arbutus menziesii*	0.296	6.71	0.146
Coast live oak (QUAG)	*Quercus agrifolia*	0.302	4.91	0.117
Shreve oak (QUPA)	*Q. parvula var. shrevei*	0.183	2.64	0.101
Ponderosa pine (PIPO)	*Pinus ponderosa*	0.085	0.96	0.036
Bigleaf maple (ACMA)	*Acer macrophyllum*	0.070	0.47	0.026
Canyon live oak (QUCH)	*Quercus chrysolepis*	0.068	0.71	0
Black oak (QUKE)	*Quercus kelloggii*	0.060	0.94	0.036
Hairy Ceanothus (CEOL)	*Ceanothus oliganthus*	0.030	0.30	0.115
Valley oak (QULO)	*Quercus lobata*	0.020	0.21	0
Blueblossom (CETH)	*Ceanothus thyrsiflorus*	0.007	0.07	0

sampled and confirmed for the presence of the pathogen. Tanoaks have shown higher initial infection rates and more rapid mortality than other canker host species (Rizzo and Garbelotto, 2003; McPherson et al., 2005). We explored tanoak mortality in relation to vegetation gradients by graphical overlay and correlation analysis of plot-scale tanoak mortality with RDA axes. More formally, we investigated possible landscape controls on forest dieback by regression analysis of tanoak mortality in relation to plot-scale and site-scale environmental factors and basal area of host tree species including coast redwood, madrone, tanoak, coast live oak, Shreve oak, canyon live oak, black oak, and bay laurel.

Our analysis consisted of the following steps:

1) Normalize the dependent variable – the proportion of total tanoak basal area that was either fallen or standing dead – using an arcsine transform of the square root of proportions (Sokal and Rolf, 1995);
2) Test independent variables for normality; log transform total live basal area of all host tree species $\log_{10}$(basal area + 10);
3) Fit a first-order trend surface to the regional trend in proportion of dead tanoak basal area (R library package *spatial*). This detrending was needed to address non-stationarity in the response variable prior to regression and autocorrelation analyses. The first order model was deemed superior to second- and third order trend based on analysis-of-variance F values;
4) Fit a multivariate regression model to the de-trended data using forward and backward variable selection (AIC criterion);
5) Test regression model residuals for spatial autocorrelation. If model residuals exhibited significant spatial autocorrelation, evaluate possible simultaneous autoregressive models (SAR) using Lagrange multiplier diagnostics to identify the most appropriate form for the model (Dormann et al., 2007). We tested a range of neighborhood sizes and a weight matrix in which weights were globally standardized and divided by the number of neighbors.

Condeso and Meentemeyer (2007) showed that *P. ramorum* disease severity is related to both fine-scale environmental factors such as microclimate and landscape-scale variables such as the area of closed forest cover up to distances of several hundred meters. We hypothesized that tanoak mortality would show stronger association with foliar hosts such as bay laurel or tanoak at the site-scale (ca. 1 ha) than at the plot scale given the ability of *P. ramorum* to disperse tens to several hundred meters from infected foliar hosts. To probe the effect of scale we repeated the regression analyses at both plot (n = 235) and site (n = 46) scales for samples containing tanoak.

3. Results

3.1. Regional host community patterns

Compared to the 280 SOD-AMP plot locations, central plots at our 58 sites were slightly lower for mean growing degree day sums (GDD5 = 3091 vs. 3128, t_{81} = 2.669, p < 0.01), higher for minimum temperature (T_{min} = 2.1 °C vs. 1.2 °C, t_{81} = 4.23, p < 0.01) and lower for temperature seasonality (T_{seas} = 17.9 vs. 20.8, t_{79} = 2.71, p < 0.01). Tanoak was present at 37/58 (63.7%) of center plots used to locate arrays and at 46/58 (79%) of sites. Because we oversampled SOD-AMP mixed-evergreen forest points with tanoak present, more plots fell closer to the coast at mid-elevations under slightly more maritime climatic conditions compared to mixed-evergreen forest as a whole in the region. Other variables such as mean annual precipitation or local solar radiation and annual heat load

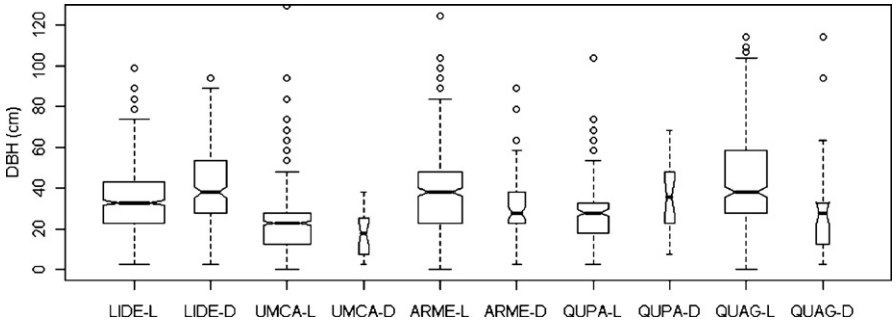

Fig. 5. Boxplots showing the distribution of stem dbh in 398 plots for the five most abundant broadleaf evergreen tree species in Big Sur mixed-evergreen forests including tanoak (LIDE), bay laurel (UMCA), madrone (ARME), Shreve oak (QUPA) and Coast live oak (QUAG). Live (-L) and dead (-D) stem size are plotted separately. Boxes show mean, quartiles, data range and data outliers. Box width is proportional to the square root of the number of observations. Non-overlapping notches indicate significantly different distributions based on a multiple comparison among means.

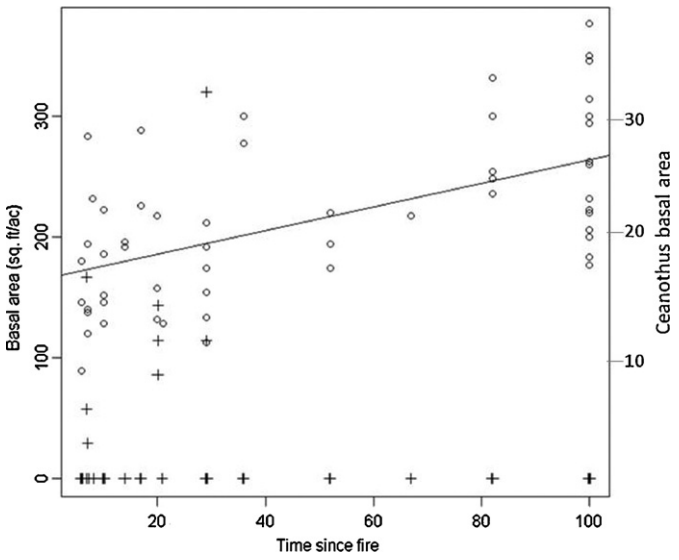

Fig. 6. Scatterplot of average site basal area (o) and basal area of Ceanothus spp. (+) as a function of time since fire. The equation for the fitted regression line is site BA = 165.82 + 0.98 × TSF; $r^2 = 0.33$, $p \ll 0.001$.

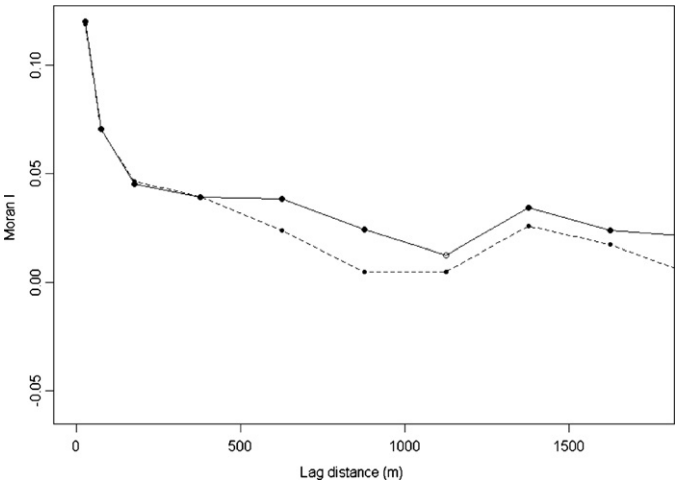

Fig. 7. Mantel correlogram showing vegetation similarity as a function of inter-plot separation for 398 mixed-evergreen basal area plots using total live plus dead basal area (solid line) and live basal area (dashed line). Data were first de-trended with redundancy analysis using easting and northing as predictor variables to remove a modest northwest-southeast trend in vegetation composition.

did not differ significantly between our plots and all SOD-AMP plots ($p > 0.10$).

The fire history of our sites was comparable to the region as a whole in terms of fraction burned in the past decade (25.4% vs. 22.6%) or burned within two decades (38.2% vs. 39.7%). Our sample included fewer areas that had not burned since 1950 (5.2% of plots vs. 38.8% of the region). This discrepancy is mainly due to limited sampling in the study area north of Point Sur, where fire frequency is much lower than in the rest of the region (Fig. 4).

Basal area data from 398 plots included 3986 stems from 14 tree species (Table 2). Sample plots ranged from 94 to 1158 m elevation and up to 9.25 km from the coast. Tanoak and coast redwood contributed the greatest basal area, followed by bay laurel, madrone, coast live oak and Shreve oak (Table 2). Species' regional frequency was highly correlated with mean local species abundance at both plot ($r = 0.96$) and site ($r = 0.89$) scales. Species richness averaged 3.65 spp. (median = 3 spp.) at the plot scale and 4.47 (median 4 spp.) at the site-scale.

Tanoak recorded the highest proportion of dead basal area (0.26), although the proportion of dead basal area exceeded 0.10 for four other dominant tree species (Table 2). Dead stems were significantly larger than living stems for tanoak (Wilcoxon rank sum test $p \ll 0.001$) and Shreve oak ($p = 0.03$) (Fig. 5). In contrast, dead stems were significantly smaller than live stems for madrone ($p < 0.01$) and coast live oak ($p \ll 0.001$) (Fig. 5).

Total basal area increased significantly with time-since-fire but there was large scatter in the relationship at both plot (adj. $r^2 = 0.16$) and site (adj. $r^2 = 0.33$) scales (Fig. 6). Mean basal area in plots less than 2 years after fire averaged 63% of plots that had no recorded burns in the previous century.

Eight of 28 sites that had burned in the previous 30 years were dominated or co-dominated by *Ceanothus oliganthus* or *C. thyrsiflorus* (Fig. 6). Although our sampling protocol was not ideal for sampling this vegetation type, we recorded maximum ceanothus basal area in plots that had burned 20–40 years ago (Fig. 6). Neither species was recorded in plots where the most recent fire occurred more than 30 years earlier, although we observed dead ceanothus stems in the understory of several older plots.

Redundancy analysis based on geographic easting and northing indicated a modest northwest-southeast trend in plot composition that accounted for 7.3% of the variance in the community data ($F = 15.86$, df = 2395; $p < 0.005$). RDA axis 1 (northwest-to-southeast) was highly correlated with minimum temperature ($r = 0.51$), growing degree days ($r = -0.64$), and time since burning (0.48); axis 2 (interior-to-coast) was correlated with minimum temperature ($r = -0.43$), temperature seasonality (−0.55) and mean annual precipitation ($r = -0.49$). Species that decreased from northwest to southeast ($p < 0.05$) included ponderosa pine, canyon live oak, Shreve oak, and coast redwood. Species that increased to the southeast included coast live oak, black oak, valley oak, and bay laurel.

Forest composition varied over short distances and plot pairs within the same site were often as different as plot pairs separated by kilometers. After regional de-trending, a low but significant positive spatial autocorrelation in plot composition was detected to distances of up to 1500 m, but Moran's I dropped steeply to less than 0.10 within the first 50–100 m (Fig. 7). The same analysis using only live basal area yielded a very similar correlogram but with a systematically lower positive autocorrelation at distances greater than 400 m. The decrease in Moran's I was due to the relatively high mortality of tanoak. Because tanoak occurred across a broader range of environments than the other tree species in the plots, its reduction increased the difference between plots at longer separation distances.

Permutation-based selection of environmental variables for redundancy analysis retained five variables including mean annual precipitation ($p < 0.01$), temperature seasonality ($p < 0.01$), growing degree days ($p < 0.01$), minimum temperature ($p < 0.01$) and time since fire ($p < 0.05$). These five variables explained 25% of the total variance, with temperature variables (minimum temperature, growing degree days, and temperature seasonality) explaining most of the variance (19.5%). As noted above, some environmental variables were highly correlated, as evidenced in the RDA biplot (Fig. 8). An RDA based only on growing degree days, temperature seasonality and time since fire explained 18.5% of the variance but resulted in a very similar scoring of plots. We show the five-factor RDA biplot to help visualize the correlations among species relative basal area and the larger set of environmental variables.

With the exception of coast redwood and bay laurel, the most common species in the plots are widely separated in the ordination space (Fig. 8). Redwood and bay laurel score highest in plots with more maritime climates (higher minimum temperatures and lower temperature seasonality) (Fig. 8). Coast live oak increases

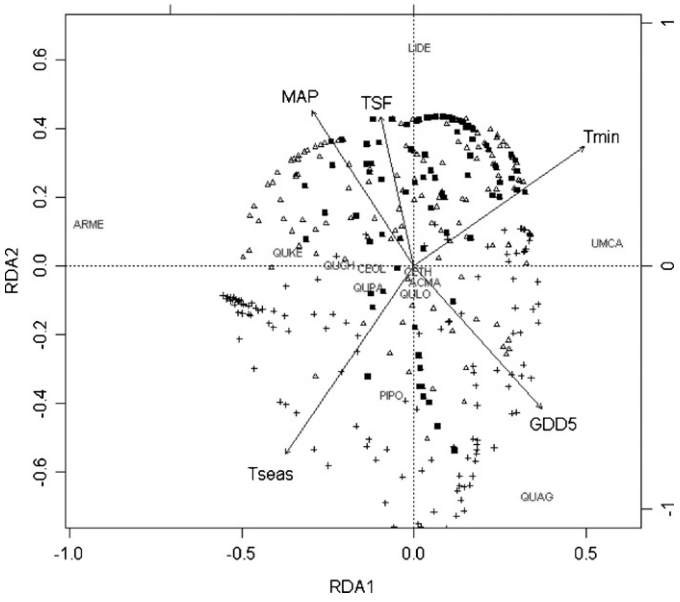

Fig. 8. Species-environment biplot of plot and species scores based on redundancy analysis (RDA) of Hellinger-transformed basal area in 398 plots. The RDA captures 24% of total variance, and the first two RDA axes account for 87% of the variance in the constrained axes. See Table 2 for code to four-letter species abbreviations. Environmental factors include average minimum daily temperature of the coldest month (T_{min}), Growing degree days above 5 °C (GDD5), mean annual precipitation (MAP), temperature seasonality (T_{seas}), and time since fire (TSF). Plot symbols show tanoak mortality patterns in relation to vegetation composition: (△) percentage of dead tanoak exceeded 25% of total tanoak basal area, (*wa*) tanoak mortality < 25%; (+) tanoak absent from plot.

Table 3
Chi-square test of association between species occurrence and mapped soil type at 58 sampling sites.

Species		Chi-square	df	*p*
Bigleaf maple	*Acer macrophyllum*	7.42	9	0.593
Madrone	*Arbutus menziesii*	15.62	9	0.073
Hairy ceanothus	*Ceanothus oliganthus*	24.5	9	0.003
Blueblossom	*Ceanothus thyrsiflorus*	3.65	9	0.93
Tanoak	*Lithocarpus densiflorus*	23.52	9	0.005
Ponderosa pine	*Pinus ponderosa*	17.51	9	0.041
Coast live oak	*Quercus agrifolia*	17.26	9	0.045
Canyon live oak	*Quercus chrysolepis*	20.67	9	0.014
Black oak	*Quercus kelloggii*	25.51	9	0.002
Valley oak	*Quercus lobata*	50.23	9	<0.001
Shreve oak	*Quercus parvula var shrevei*	8.08	9	0.526
Coast redwood	*Sequoia sempervirens*	26.29	9	0.002
Bay laurel	*Umbellularia californica*	17.45	9	0.042

at higher growing degree days. Madrone is clearly associated with high precipitation but also high temperature seasonality. Tanoak is somewhat distinctive in its association with longer time since fire and higher mean annual precipitation, although the species was encountered across a broad spectrum of environments and vegetation composition (Fig. 8).

3.2. Species response models

Sampling sites fell on 10 different mapped soil series. Although 46/58 sites were mapped as either Gamboa-Sur complex, Sur-Junipero complex, or Junipero sandy loam, occurrence of most tree species was significantly associated with specific soil types (Table 3). This includes valley oak, which occurred in only six plots at four sites but was strongly associated with the Mills-Gatos com-

Table 4
Non-parametric multiplicative regression (NPMR) models for dominant tree and shrub species in mixed-evergreen forest sites ($n = 58$ sites). Factors selected in the best 1-,2-, and 3-factor models and cross-validated pseudo-R^2 goodness-of-fit statistics are tabulated. Selected factors include mean annual precipitation (MAP), area of watershed draining through the site (flow.accum), time since fire in years (TSF), average minimum temperature of the coldest month (TMIN), average maximum temperature of the warmest month (TMAX), and calculated annual heatload (heat.load). See Section 2 for a more detailed explanation of environmental factors.

Species		Factor 1	Factor 2	Factor 3	Pseudo-R^2
Bigleaf maple	*Acer macrophyllum*	MAP			0.07
		MAP	flow.accum		0.11
Madrone	*Arbutus menziesii*	GDD5			0.45
		GDD5	T_{seas}		0.67
		GDD5	T_{seas}	T_{min}	0.74
Hairy ceanothus	*Ceanothus oliganthus*	GDD5			0.25
		GDD5	TSF		0.32
		GDD5	TSF	Solar.rad	0.53
Tanoak	*Lithocarpus densiflorus*	GDD5			0.27
		GDD5	Heat.load		0.33
Ponderosa pine	*Pinus ponderosa*	T_{seas}			0.27
		T_{seas}	TSF		0.55
		T_{seas}	TSF	Flow.accum	0.60
Coast live oak	*Quercus agrifolia*	GDD5			0.25
		GDD5	Heat.load		0.36
		GDD5	Heat.load	MinT	0.43
Canyon live oak	*Quercus chrysolepis*	MinT			0.05
		MinT	Heat.load		0.25
Black oak	*Quercus kelloggii*	GDD5			0.29
		GDD5	Solar.irrad		0.65
Shreve oak	*Quercus parvula*	T_{seas}			0.16
		T_{seas}	Heat.load		0.25
Coast redwood	*Sequoia sempervirens*	T_{min}			0.25
		T_{min}	Solar.rad		0.36
Bay laurel	*Umbellularia californica*	T_{min}			0.08
		T_{min}	MAP		0.18

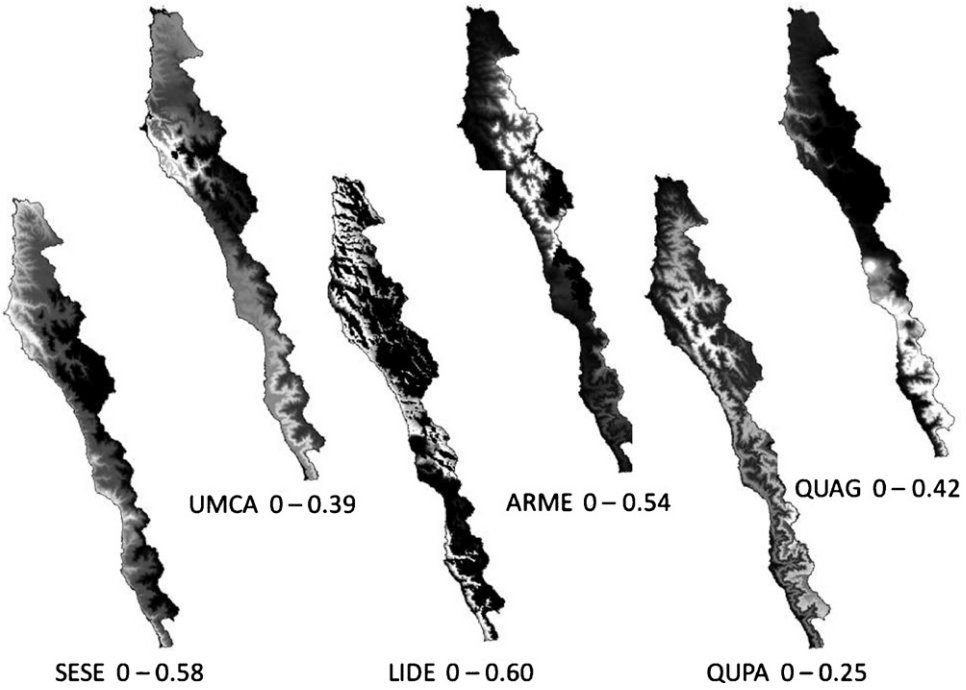

Fig. 9. Species distribution models for six dominant tree species associated with mixed-evergreen forest in the Big Sur Region, California, including from left to right: Coast redwood (*Sequoia sempervirens)* [SESE]; Bay laurel (*Umbellularia californica)* [UMCA]; Tanoak (*Lithocarpus densiflorus*) [LIDE]; Madrone (*Arbutus menziesii)* [ARME]; Shreve oak (*Quercus parvula*)[QUPA], and coast live oak (Quercus agrifolia)[QUAG]. Numbers below species abbreviations are the range of probabilities represented by the grey scale maps from low (black) to high (white). Models are based on Non-parametric Multiplicative Regression models (Table 4) and 90 m GIS data (Fig. 4).

plex and Sur-Plaskett complex soils (Table 3). The only species not significantly associated with mapped soil types were bigleaf maple, madrone, blueblossom and Shreve oak. Relative basal area of several species was significantly ($p < 0.05$) correlated with higher soil available water holding capacity (AWC), notably coast live oak, tanoak and redwood, while other species including Shreve oak and canyon live oak were associated with shallower soils and lower AWC.

For the 11 most frequent species, single-factor models or two-factor models are comparable or only slightly inferior to three-factor models (Table 4). Pseudo-R^2 values for two-factor models of <0.25 indicate relatively poor model fits for canyon live oak, Shreve oak and bay laurel. Models are stronger for the remaining species with especially good fits for madrone, ponderosa pine and black oak, all of which tend to increase at higher elevations away from the coast. No two species are associated with the same combination of factors. GDD5 is the most frequently selected variable, appearing in 5 of 11 two-factor species models. Madrone, tanoak and black oak abundance are highest at intermediate values of GDD5 whereas coast live oak increases at higher levels of GDD5. Coast redwood and bay laurel increase in more maritime temperature regimes (higher minimum temperatures) while canyon live oak attains highest relative basal area at more interior, higher elevations with low minimum temperatures.

Species distributions are not readily summarized along a single environmental gradient, but broad coast-to-interior and north-to-south patterns are obvious in the tree species distribution models (Fig. 9).

Most species do not show strong, consistent relationships to time since fire, which appears as the second term in NPMR models for hairy ceanothus and ponderosa pine (Table 4). Ponderosa pine is associated with higher fire frequency and short time since fire, and hairy ceanothus relative basal area peaks at 30–35 years after fire. Goodness-of-fit r^2 values for univariate linear regression models of species relative basal area as a function of TSF range from <0.01 to 0.06. Psuedo-R^2 values for univariate NPMR models range from 0 to 0.16.

Local topographic variation within a site explains a small amount of additional variation in species relative basal area. After accounting for site mean basal area, madrone increases in plots with higher radiation load ($r^2 = 0.13$, $p = 0.009$), black oak increases in plots with lower topographic moisture index ($r^2 = 0.30$, $p < 0.001$), and redwood increases in plots with higher topographic moisture index ($r^2 = 0.02$, $p = 0.04$).

3.3. Tanoak mortality patterns

Tanoak dieback ranged from 0 to 100% of tallied trees and was most widespread in the northern part of the study area in Bixby Creek, Little Sur River, Big Sur River and Ventana Creek watersheds (Fig. 10). Percent dead basal was generally lower at more interior locations, especially in the northern half of the study area where plots ranged further from the coast.

3.3.1. Plot-scale analysis

Overlay of tanoak mortality data on the RDA plot illustrates that high (>25% of total basal area) tanoak mortality was observed across a wide range of environmental conditions and forest composition, and was correlated with high mean annual precipitation and long time since fire (Fig. 8).

A first-order trend surface fit a significant west-to-east gradient of decreasing proportion of dead tanoak basal area (adj. $r^2 = 0.25$, $F = 33.66$, $p \ll 0.0001$; Fig. 10). The trend surface was significantly correlated (Kendall's test, $p < 0.05$) with mean annual precipitation ($r = 0.65$), growing degree days ($r = -0.29$), minimum temperature ($r = 0.27$), temperature seasonality ($r = -0.47$), annual solar radiation ($r = -0.34$) and annual heat load ($r = -0.23$).

De-trended tanoak mortality was significantly correlated with total basal area of bay laurel ($r = 0.29$, $p < 0.001$) and except for tanoak was unrelated to basal area of other host species (Table 5).

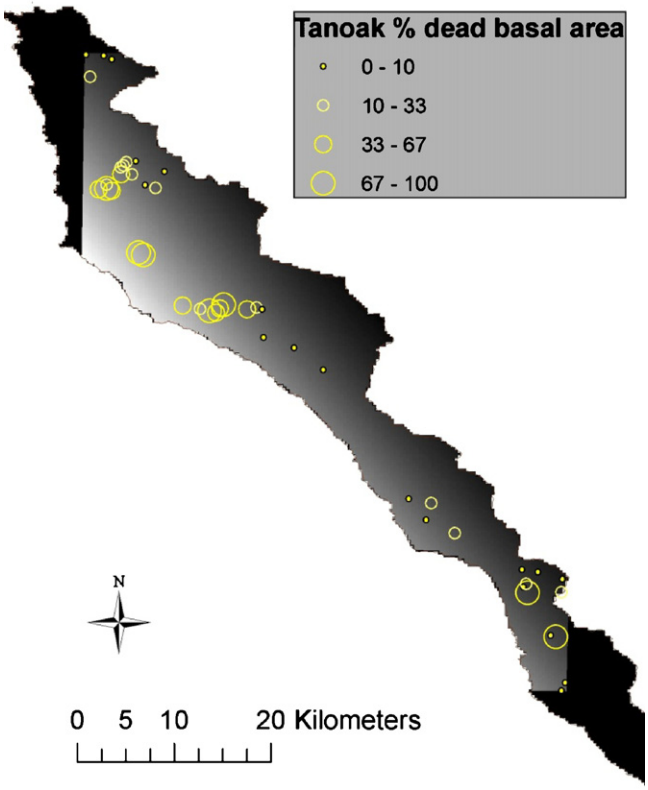

Fig. 10. Spatial pattern in tanoak (*Lithocarpus densiflorus*) mortality at 46 sites in the Big Sur region, Spring 2006. Circles are proportional to percent of total basal area tallied as standing or down dead. The grayscale shows the first-order trend surface fitted to 235 plots using the arcsin transform of the square root of percentage data (adjusted $r^2 = 0.26$), with darker shades indicating lower values (black areas to the north and south are beyond the geographic range of the data).

This same result was obtained for tanoak mortality data that were not de-trended.

Linear regression on log-transformed bay laurel basal area and GDD5 explained an additional 12% of the variance in de-trended proportion dead basal area ($p < 0.0001$, Table 6). Regression residuals exhibited low but marginally significant spatial autocorrelation (Moran's $I = 0.019$, $p = 0.05$) (Table 6). Several spatial autoregressive models were tested but were rejected based on LaGrange multiplier diagnostic tests (Dormann et al., 2007).

3.3.2. Site-level analysis

De-trended tanoak mortality was significantly correlated with site basal area of bay laurel ($r = 0.54$, $p < 0.0001$), negatively correlated with total tanoak basal area ($r = -0.30$, $p = 0.05$), and unrelated to basal area of other host species (Table 6). The first order trend surface (adj. $r^2 = 0.20$, $F_2 = 6.78$, $p = 0.003$; Fig. 10) was significantly correlated with mean annual precipitation ($r = 0.62$), minimum temperature ($r = 0.30$), growing degree days ($r = 0.32$), temperature seasonality ($r = -0.51$), solar radiation ($r = -0.38$) and annual heat-load ($r = -0.34$).

Site basal area of bay laurel was the only variable retained in stepwise regression against the de-trended proportion of dead tanoak basal area (adj. $r^2 = 0.28$, $F_{1,44} = 18.26$, $p \ll 0.001$; Table 6). Model residuals were not significantly spatially autocorrelated (Moran's $I = -0.06$, $p = 0.68$).

Table 5
Correlation of tanoak mortality with total basal area of other host tree species at both plot and site-scales. Host basal areas were transformed using $\log_{10}$(basal area + 10). Proportion of dead tanoak basal area was transformed using arcsin($p^{0.5}$).

Species		Plot scale $n = 235$	Site-scale $n = 36$
Madrone	*Arbutus menziesii*	−0.083	−0.16
Tanoak	*Lithocarpus densiflorus*	−0.061	−0.30*
Coast live oak	*Quercus agrifolia*	0.088	0.23
Canyon live oak	*Quercus crysolepis*	−0.073	−0.11
Black oak	*Quercus kelloggii*	−0.106	−0.17
Shreve oak	*Quercus parvula*	0.104	0.22
Coast redwood	*Sequoia sempervirens*	−0.070	−0.07
Bay laurel	*Umbellularia californica*	0.292***	0.54***

* $p < 0.05$.
*** $p < 0.0001$.

4. Discussion

4.1. Forest composition and environmental associations

Forests dominated by broadleaved, sclerophyllous evergreen trees occur in Mediterranean climate regions from southern Oregon to northern Baja Mexico. Vegetation ecologists have generally viewed these forests as transitional between chaparral on hotter, drier sites that increase south of central coastal California, and conifer forests on cooler, mesic sites that increase to the north (Cooper, 1922; Whittaker, 1960; Wells, 1962; Peinado et al., 1997). Some dominant members of the mixed-evergreen forest – notably tanoak and madrone – are also important understory components of mature Douglas fir (*Pseudotsuga menziesii*) and mixed-conifer forests, and much of the research on these species has been motivated by timber management in conifer-dominated ecosystems (Tappeiner and McDonald, 1984). The mixed-evergreen forest of the Big Sur region is distinctive from related forests to the north and south: Plot- and site-scale tree diversity is higher than forests further south (2–5 spp. vs. 1–2 spp.). With the exception of redwood, which tends to segregate locally in wetter ravines and lower hillslopes, the forest here generally lacks constituent conifer species of forests further north.

Mixed-evergreen forest in the study area is patchily distributed and most extensive in the northern end of the region, on north facing slopes, at mid-elevations near the coast. The region presents a complex array of biophysical environments; climate, geology, soils and fire regime here can be highly correlated and their effects on species' distributions are difficult to tease apart based on observational data. Nevertheless, multi-species forest composition analyzed by redundancy analysis and individual species distributions analyzed using non-parametric multiplicative regression both suggest significant climate control on mixed-evergreen forest composition in the Big Sur Region. The 90 m climate grids used here are two orders of magnitude higher spatial resolution than relatively high-resolution (~1 km) climate grids more commonly used for species distribution modeling (e.g., Kueppers et al., 2005; Rehfeldt et al., 2006; Loarie et al., 2009). The 90 m resolution proved especially important in resolving the strongly contrasting and locally inverted temperature regimes associated with the marine boundary layer near the coast, and for approximating the sampling scale of our site arrays. Choice of spatial scale is critical in analyzing species–environment associations (Wiens, 1989) and a central problem in bioclimate modeling (Guisan and Thuiller, 2005). We are encouraged by the performance of the high resolution grids used here, especially given the relatively sparse network of weather stations in the region.

Relative basal area of the dominant tree species turns over steeply from north to south and from coast to interior in a pattern consistent with temperature and soil moisture controls proposed by Waring and Major (1964). Species sort along coast-to-interior gradients of increasing continentality (lower minimum temperatures and higher temperature seasonality), increasing precipitation and decreasing time since fire. Species also sort along north-to-

Table 6
Regression results for the effects of location, environmental factors and basal area of bay laurel on regionally de-trended tanoak mortality in mixed-evergreen forests of the Big Sur region, California. Models include plot scale and site-scale. The dependent variable is 2/pi*arcsin((fraction dead basal area)0.5). Independent variables include mean Growing Degree Days above 5 °C (GDD5) and log basal area of bay laurel (*Umbellularia californica*) in ft^2/ac (log*UMCA*). Moran's *I* values measure the level of spatial autocorrelation of model residuals and adjusted r^2 measures model goodness-of-fit.

Model scale	Sample size	Intercept	log*UMCA*	GDD5	Moran's *I*	Adj r^2
Plot	235	$-2.3657 \pm 0.5528^{****}$	$0.2125 \pm 0.0529^{****}$	$5.613e-04 \pm 1.508e-04^{**}$	0.019^{*}	0.12^{***}
Site	46	$-0.50826 \pm 0.1237^{***}$	$0.2599 \pm 0.0608^{***}$		−0.06	0.2772^{**}

* $p < 0.05$.
** $p < 0.01$.
*** $p < 0.001$.
**** $p < 0.0001$.

south gradients of increasing growing degree days, decreasing mean annual precipitation and higher temperature seasonality. As a coarse generalization, species can be ordered along a complex gradient from high minimum soil moisture/maritime temperature regime to lower minimum soil moisture/continental temperature regime: coast redwood > bay laurel > tanoak > coast live oak > Shreve oak > canyon live oak > black oak > madrone (Note: coast live oak and shreve oak were sometimes difficult to distinguish both in the field and in terms of their ecological affinities). Lacking direct measurements, we view this simplistic, one dimensional ordering as a hypothesis to be tested and refined by more detailed microclimate and soil monitoring.

We were not able to explain much of the large within-site variation in forest composition. Local topographic terms (heat load, solar radiation, flow accumulation) were the second term in six of 12 species models, suggesting a hierarchy of environmental controls from large-scale climate factors to more local topo-climatic influences. For a few species, notably black oak, Shreve oak and coast redwood, additional within-site variation was partly explained by micro-topographic variation in solar radiation, heat load and flow accumulation patterns. In retrospect, our investigation would have benefitted from more detailed characterization of local geomorphic and soil conditions. Most tree species are strongly associated with mapped soils and much soil variation exists within the mapped soil units due to local landslides, slumps and other hillslope processes.

The fire ecology of mixed-evergreen forests is not well studied. It appears that mixed-evergreen forest in the Big Sur region experiences a mixed-fire regime ranging from low severity understory burns to high severity crown fires, with the latter increasing above the marine inversion layer and at more interior locations. Excluding valley oak, which was rare in our samples, all dominant broadleaved species are vigorous stump sprouters after fire or cutting, so one would expect mixed-evergreen forest to be relatively resilient under a mixed-severity fire regime (Donato et al., 2009). Nevertheless, in the Santa Lucia Ranges mixed-evergreen forest can be at least temporarily replaced by ceanothus chaparral, especially on more xeric sites. We sampled several recent burns dominated by *Ceanothus oliganthus* or *C. thyrsiflorus* but still retaining scattered mature tanoaks that survived the burn, and also sampled several stands with dead ceanothus stems in the understory of mixed-evergreen forest. Both ceanothus species are obligate seeding members of the genus and have been described as short-lived (Keeley, 1983; Ford and Hayes, 2007). The transient dominance of forest sites by ceanothus chaparral contradicts Cooper's (1922) view that chaparral and mixed-evergreen forest are topographically controlled local climax types with no successional relationship to one another in the region.

We found a weak relationship between relative species abundance and fire history but that is partly due to our sampling design. Fire size and frequency increase moving southward and away from the coast, so that we could not obtain a comparable range of fire histories throughout the region. Furthermore, because we only sampled the mixed-evergreen forest stratum, we did not systematically sample sites currently dominated by chaparral or other types that might have supported mixed-evergreen forest prior to severe burning within the past few decades.

Better understanding of fire regime controls on vegetation is critical given the possibility of increased fire severity in areas with high tree mortality. Fire severity patterns after the 2008 Basin Complex fires suggest a complex relationship between disease impacts and fire behavior in which infected trees are more likely to be killed by fire and fire severity varies depending on the stage of disease progression and associated fuel structures (e.g., amount of standing vs. downed material) (Metz et al., in review). Spatial variation in burn severity, pre-burn patterns in seed banks of fire-following Ceanothus species, and fire-caused seed and sprout mortality across this complex vegetation mosaic could produce an extremely wide range of outcomes in post-burn vegetation.

4.2. Spatial variation in tanoak mortality

Eight of nine tree species in our plots are either foliar or canker hosts to *P. ramorum*. Forest dieback is now extensive, although the proportion of dead basal area is still highest in northern canyons (Meentemeyer et al., 2008c). We recorded relatively high mortality in canker-forming hosts tanoak, coast live oak and Shreve oak and in the foliar host bay laurel. The large number of standing and recently fallen mature stems of tanoaks is consistent with *P. ramorum* impacts reported by other investigators in central California (McPherson et al., 2005; Meentemeyer et al., 2008c; Brown and Allen-Diaz, 2009). Dead tanoaks and coast live oaks were significantly larger than live individuals, a result in agreement with McPherson et al. (2005) who found that the mean diameter of symptomatic tanoaks and coast live oaks in Marin County study plots was greater than asymptomatic individuals.

Tanoak dieback is catalyzed by bay laurel and the influence of bay laurel extends beyond the immediate forest neighborhood, so that site-level basal area of bay laurel (ca. 1 ha scale) better predicts plot-scale (ca. 0.05 ha) tanoak dieback than bay laurel basal area in the plot. This result is not unexpected given documented dispersal of *P. ramorum* up to several hundred meters or more from infected bay laurel (Davidson et al., 2005; Mascheretti et al., 2008). It also supports the conclusion by Condeso and Meentemeyer (2007) that disease severity – which in their study was measured by the number of symptomatic leaves on bay laurel stems – increases at the plot scale as the source of innoculum (bay laurel) increases in the surrounding area.

Inference about environmental and biotic controls on forest dieback is complicated by several factors: climatic factors such as precipitation and temperature that have been associated with disease prevalence vary systematically from north to south and from coast to interior locations; foliars host such as bay laurel that have been associated with the disease vary in abundance along regional and local gradients; and, the disease is probably still dispersing across the region.

Regression model results indicate that the incidence and severity of the disease is coupled to landscape and regional patterns in biophysical environments and associated forest composition, supporting previous efforts to model disease risk using factors such as bioclimatic factors and species distribution models (Meentemeyer et al., 2004). Adaptive management of mixed-evergreen forest to mitigate *P. ramorum* impacts in the region will need to consider large local and regional variation in forest composition and the potentially strong interactions between climate, fire, forest composition and disease severity.

Acknowledgements

Research funding was provided by the USDA Forest Service Joint Venture Agreement No. 05-JV-11272138-059 and NSF EF-0622770. The authors thank Allison Wickland, Kerri Frangioso, Jason Kreitler, Patrick Jantz, and Theresa Nogeire for their help collecting field data. We gratefully acknowledge administrative support from staff at UCSB's Institute for Computational Earth System Science.

References

Blanchet, F.G., Legendre, P., Borcard, D., 2008. Forward selection of explanatory variables. Ecology 89, 2623–2632.
Borcard, D., Legendre, P., Avois-Jacquet, C., Tuomisto, H., 2004. Dissecting the spatial structure of ecological data at multiple scales. Ecology 85, 1826–1832.
Brown, L.B., Allen-Diaz, B., 2009. Forest stand dynamics and sudden oak death: mortality in mixed-evergreen forests dominated by coast live oak. Forest Ecology and Management 257, 1271–1280.
Cal Fire, 2006. Fire perimeters database. California Department of Forestry and Fire Protection, http://frap.cdf.ca.gov/data/frapgisdata/download.asp?spatialdist=1&rec=fire.
Castello, J.D., Leopold, D.J., Smallidge, P.J., 1995. Pathogens, patterns, and processes in forest ecosystems. Bioscience 45, 16–24.
Chornesky, E.A., Bartuska, A.M., Aplet, G.H., Britton, K.O., Cummings-Carlson, J., Davis, F.W., Eskow, J., Gordon, D.R., Gottschalk, K.W., Haack, R.A., Hansen, A.J., Mack, R.N., Rahel, F.J., Shannon, M.A., Wainger, L.A., Wigley, T.B., 2005. Science priorities for reducing the threat of invasive species to sustainable forestry. Bioscience 55, 335–348.
Cobb, R.C., Meentemeyer, R.K., Rizzo, D.M., 2010. Apparent competition in canopy trees determined by pathogen transmission rather than susceptibility. Ecology 91 (2), 327–333.
Condeso, T.E., Meentemeyer, R.K., 2007. Effects of landscape heterogeneity on the emerging forest disease sudden oak death. Journal of Ecology 95, 364–375.
Cooper, W.S., 1922. The Broad-Sclerophyll Vegetation of California. Carneggie Institute of Washington, Washington DC.
Daly, C., Halbleib, M., Smith, J.I., Gibson, W.P., Doggett, M.K., Taylor, G.H., Curtis, J., Pasteris, P.P., 2008. Physiographically sensitive mapping of climatological temperature and precipitation across the conterminous United States. International Journal of Climatology 28, 2031–2064.
Davidson, J.M., Wickland, A.C., Patterson, H.A., Falk, K.R., Rizzo, D.M., 2005. Transmission of *Phytophthora ramorum* in mixed-evergreenforest in California. Phytopathology 95, 587–596.
Davidson, J.M., Patterson, H.A., Rizzo, D.M., 2008. Sources of inoculum for *Phytophthora ramorum* in a redwood forest. Phytopathology 98, 860–866.
Davis, F.W., Borchert, M., 2006. Central coast bioregion. In: Sugihara, N.G., Van Wagtendtonk, J.W., Shaffer, K.E., Fites-Kaufman, J., Thode, A.E. (Eds.), Fire in California's Ecosystems. University of California, Berkeley, California, pp. 321–349.
Donato, D.C., Fontaine, J.B., Robinson, W.D., Kauffman, J.B., Law, B.E., 2009. Vegetation response to a short interval between high-severity wildfires in a mixed-evergreen forest. Journal of Ecology 97, 142–154.
Dormann, C.F., McPherson, J.M., Araujo, M.B., Bivand, R., Bolliger, J., Carl, G., Davies, R.G., Hirzel, A., Jetz, W., Kissling, W.D., Kuhn, I., Ohlemuller, R., Peres-Neto, P.R., Reineking, B., Schroder, B., Schurr, F.M., Wilson, R., 2007. Methods to account for spatial autocorrelation in the analysis of species distributional data: a review. Ecography 30, 609–628.
Farr, T.G., Rosen, P.A., Caro, E., Crippen, R., Duren, R., Hensley, S., Kobrick, M., Paller, M., Rodriguez, E., Roth, L., Seal, D., Shaffer, S., Shimada, J., Umland, J., Werner, M., Oskin, M., Burbank, D., Alsdorf, D., 2007. The shuttle radar topography mission. Reviews of Geophysics 45, RG2004, 33 p.
Finch, H.D.S., 1957. Plotless enumeration with angle gauges. Forestry 30, 173–192.
Flint, A.L., Flint, L.E, 2007. Application of the basin characterization model to estimate in-place recharge and runoff potential in the Basin and Range carbonate-rock aquifer system, White Pine County, Nevada, and adjacent areas in Nevada and Utah. U.S. Geological Survey Scientific Investigations Report 2007-5099.
Ford, L.D., Hayes, G.F., 2007. Northern coastal scrub and coastal prairie. In: Barbour, M.G., Keeler-Wolf, T., Schoenherr, A.A. (Eds.), Terrestrial Vegetation of California, 3rd ed. University of California, Berkeley, California, pp. 179–207.
Goslee, S.C., Urban, D.L., 2007. The ecodist package for dissimilarity-based analysis of ecological data. Journal of Statistical Software 22, 19.
Guisan, A., Thuiller, W., 2005. Predicting species distribution: offering more than simple habitat models. Ecology Letters 8, 993–1009.
Hall, B., Motzkin, G., Foster, D.R., Syfert, M., Burk, J., 2002. Three hundred years of forest and land-use change in Massachusetts, USA. Journal of Biogeography 29, 1319–1335.
Hastie, T.J., Tibshirani, R.J., 1986. Generalized additive models. Statistical Science 1, 297–318.
Holdenrieder, O., Pautasso, M., Weisberg, P.J., Lonsdale, D., 2004. Tree diseases and landscape processes: the challenge of landscape pathology. Trends in Ecology & Evolution 19, 446–452.
Holzmueller, E.J., Jose, S., Jenkins, M.A., 2008. The relationship between fire history and an exotic fungal disease in a deciduous forest. Oecologia 155, 347–356.
Hunter, J.C., Parker, V.T., 1993. The disturbance regime of an old-growth forest in coastal California. Journal of Vegetation Science 4, 19–24.
Johnson, A.C., Wilcock, P., 2002. Association between cedar decline and hillslope stability in mountainous regions of southeast Alaska. Geomorphology 46, 129–142.
Keeley, J.E., 1983. Longevity of nonsprouting Ceanothus. American Midland Naturalist 93, 504–507.
Kueppers, L.M., Snyder, M.A., Sloan, L.C., Zavaleta, E.S., Fulfrost, B., 2005. Modeled regional climate change and California enaemic oak ranges. Proceedings of the National Academy of Sciences of the United States of America 102, 16281–16286.
Legendre, P., Gallagher, E.D., 2001. Ecologically meaningful transformations for ordination of species data. Oecologia 129, 271–280.
Loarie, S.R., Duffy, P.B., Hamilton, H., Asner1, G.P., Field, C.B., Ackerly, D.D., 2009. The velocity of climate change. Nature 462, 1052–1055.
Loo, J., 2009. Ecological impacts of non-indigenous invasive fungi as forest pathogens. Biological Invasions 11, 81–96.
McCune, B., 2006. Non-parametric habitat models with automatic interactions. Journal of Vegetation Science 17, 819–830.
Mascheretti, S., Croucher, P.J.P., Vettraino, A., Prospero, S., Grabelotto, M., 2008. Reconstruction of the sudden oak death epidemic in California through microsatellite analysis of the pathogen *Phytophthora ramorum*. Molecular Ecology 17, 2755–2768.
McCune, B., 2007. Improved estimates of incident radiation and heat load using non-parametric regression against topographic variables. Journal of Vegetation Science 18, 751–754.
McCune, B., Mefford, M.J., 2004. Hyperniche. Multiplicative Habitat Modeling. MjM Software, Gleneden Beach, Oregon, USA.
McPherson, B.A., Mori, S.R., Wood, D.L., Storer, A.J., Svihra, P., Kelly, N.M., Standiford, R.B., 2005. Sudden oak death in California: disease progression in oaks and tanoaks. Forest of Ecology Management 213, 71–89.
Meentemeyer, R., Rizzo, D., Mark, W., Lotz, E., 2004. Mapping the risk of establishment and spread of sudden oak death in California. Forest of Ecology Management 200, 195–214.
Meentemeyer, R.K., Anacker, B.L., Mark, W., Rizzo, D.M., 2008a. Early detection of emerging forest disease using dispersal estimation and ecological niche modeling. Ecological Applications 18, 377–390.
Meentemeyer, R.K., Rank, N.E., Anacker, B.L., Rizzo, D.M., Cushman, J.H., 2008b. Influence of land-cover change on the spread of an invasive forest pathogen. Ecological Applications 18, 159–171.
Meentemeyer, R.K., Rank, N.E., Shoemaker, D.A., Oneal, C.B., Wickland, A.C., Frangioso, K.M., Rizzo, D.M., 2008c. Impact of sudden oak death on tree mortality in the Big Sur ecoregion of California. Biological Invasions 10, 1243–1255.
Metz, M. R., Frangioso, K. M., Meentemeyer, R.K., Rizzo, D.M, in review. Interacting disturbances: Wildfire severity affected by stage of forest disease invasion. Submitted to Ecological Applications.
Miles, S.R., Goudey, C.B., 1997. Ecological subregions of California: section and subsection descriptions. Report R5-EM-TP-005, USDA Forest Service, Pacific Southwest Region, San Francisco, CA.
Moore, I.D., Grayson, R.B., Ladson, A.R., 1991. Digital terrain modeling – a review of hydrological, geomorphological, and biological applications. Hydrological Processes 5, 3–30.
Peinado, M., Aguirre, J.L., Delgadillo, J., 1997. Phytosociological, bioclimatic and biogeographical classification of woody climax communities of western North America. Journal of Vegetation Science 8, 505–528.
Perkins, T.E., Matlack, G.R., 2002. Human-generated pattern in commercial forests of southern Mississippi and consequences for the spread of pests and pathogens. Forest Ecology Management 157, 143–154.
Rehfeldt, G.E., Crookston, N.L., Warwell, M.V., Evans, J.S., 2006. Empirical analyses of plant-climate relationships for the western United States. International Journal of Plant Sciences 167, 1123–1150.
Rizzo, D.M., Garbelotto, M., 2003. Sudden oak death: endangering California and Oregon forest ecosystems. Frontiers Ecology Environment 1, 197–204.
Sawyer, J.O., Thornburgh, D.A., Griffin, J.R., 1977. Mixed evergreen forest. In: Barbour, M.G., Major, J. (Eds.), Terrestrial Vegetation of California. California Native Plant Society, Sacramento, California, pp. 383–416.
Sokal, R.R., Rolf, F.J., 1995. Biometry, New York.
Tappeiner, J.C., McDonald, P.M., 1984. Development of tanoak understories in conifer stands. Canadian Journal of Forest Research – Review Canadian Recherche Forestiere 14, 271–277.
U.S. Department of Agriculture (USDA) Natural Resources Conservation Service (NRCS), 2004. Soil Survey Geographic (SSURGO) Database for Monterey County,

California, U.S. Department of Agriculture, Natural Resources Conservation Service, Fort Worth, Texas.
Waring, K.A., O'Hara, K.L., 2008. Redwood/tanoak stand development and response to tanoak mortality caused by *Phytophthora ramorum*. Forest Ecology and Management 255, 2650–2658.
Waring, R.H., Major, J., 1964. Some vegetation of california coastal redwood region in relation to gradients of moisture nutrients light + temperature. Ecological Monographs 34, 167–215.
Wells, P.V., 1962. Vegetation in relation to geological substratum and fire in San Luis Obispo Quadrangle, California. Ecology Monograph 32, 79–103.
White, M.A., Brown, T.N., Host, G.E., 2002. Landscape analysis of risk factors for white pine blister rust in the mixed forest province of Minnesota, USA. Canadian Journal of Forest Research – Review Canadian Recherche Forestiere 32, 1639–1650.
Whittaker, R.H., 1960. Vegetation of the Siskiyou Mountains. Oregon and California Ecological Monographs 30, 280–338.
Wickland, A.C., Frangioso, K.M., Rizzo, D.M., Meentemeyer, R.K., 2008. The Big Sur ecoregion sudden oak death adaptive management project: ecological monitoring. In: Frankel, S.J., Kliejunas, J.T., Palmieri, K.M. (Eds.), Sudden Oak Death Third Science Symposium. U.S. Department of Agriculture, Forest Service, Pacific Southwest Research Station, Albany, CA, pp. 489–490.
Wiens, J.A., 1989. Spatial scaling in ecology. Functional Ecology 3, 385–397.